Received: 2 September 2019 | Revised: 17 January 2020 | Accepted: 2 February 2020

DOI: 10.1111/gcb.15037

PRIMARY RESEARCH ARTICLE

Global Change Biology WILEY

A catastrophic tropical drought kills hydraulically vulnerable tree species

Jennifer S. Powers[1,2] | German Vargas G.[2] | Timothy J. Brodribb[3] | Naomi B. Schwartz[4] | Daniel Pérez-Aviles[1] | Chris M. Smith-Martin[2] | Justin M. Becknell[5] | Filippo Aureli[6,7] | Roger Blanco[8] | Erick Calderón-Morales[1] | Julio C. Calvo-Alvarado[9] | Ana Julieta Calvo-Obando[9] | María Marta Chavarría[8] | Dorian Carvajal-Vanegas[9] | César D. Jiménez-Rodríguez[9,10] | Evin Murillo Chacon[8] | Colleen M. Schaffner[7,11] | Leland K. Werden[2] | Xiangtao Xu[12,13] | David Medvigy[14]

[1]Department of Ecology, Evolution, & Behavior, University of Minnesota, St. Paul, MN, USA

[2]Department of Plant and Microbial Biology, University of Minnesota, St. Paul, MN, USA

[3]School of Biological Sciences, University of Tasmania, Hobart, Tas., Australia

[4]Department of Geography, University of British Columbia, Vancouver, BC, Canada

[5]Environmental Studies Program, Colby College, Waterville, ME, USA

[6]School of Biological and Environmental Sciences, Liverpool John Moores University, Liverpool, UK

[7]Instituto de Neuroetologia, Universidad Veracruzana, Xalapa, Mexico

[8]Programa de Investigación, Área de Conservación Guanacaste, Sistema Nacional de Areas de Conservación, Ministerio de Ambiente y Energía, Liberia, Costa Rica

[9]Escuela de Ingeniería Forestal, Tecnológico de Costa Rica, Cartago, Costa Rica

[10]Water Resources Section, Delft University of Technology, Delft, The Netherlands

[11]Psychology Department, Adams State University, Alamosa, CO, USA

[12]Department of Organismic and Evolutionary Biology, Harvard University, Cambridge, MA, USA

[13]Department of Ecology and Evolutionary Biology, Cornell University, Ithaca, NY, USA

[14]Department of Biological Science, University of Notre Dame, Notre Dame, IN, USA

Correspondence
Jennifer S. Powers, Departments of Ecology, Evolution & Behavior and Plant & Microbial Biology, University of Minnesota, St. Paul, MN 55108, USA.
Email: powers@umn.edu

Funding information
United States National Science Foundation, Grant/Award Number: DEB 1053237, NSF PRFB 1711366, CRN3025 and GrantGEO-128040; Technological Institute of Costa Rica; Chester Zoo; National Geographic Society; Consejo Nacional por la Ciencia y la Tecnología; US Department of Energy, Grant/Award Number: DESC0014363; ARC, Grant/Award Number: DP170100761

Abstract

Drought-related tree mortality is now a widespread phenomenon predicted to increase in magnitude with climate change. However, the patterns of which species and trees are most vulnerable to drought, and the underlying mechanisms have remained elusive, in part due to the lack of relevant data and difficulty of predicting the location of catastrophic drought years in advance. We used long-term demographic records and extensive databases of functional traits and distribution patterns to understand the responses of 20–53 species to an extreme drought in a seasonally dry tropical forest in Costa Rica, which occurred during the 2015 El Niño Southern Oscillation event. Overall, species-specific mortality rates during the drought ranged from 0% to 34%, and varied little as a function of tree size. By contrast, hydraulic safety margins correlated well with probability of mortality among species, while morphological or leaf economics spectrum traits did not. This firmly suggests hydraulic traits as targets for future research.

KEYWORDS

extreme drought, hydraulic traits, rainfall seasonality, tree mortality

1 | INTRODUCTION

Drought-related tree mortality is now a widespread phenomenon predicted to increase in magnitude with climate change (Allen et al., 2010), affecting trees in boreal (Peng et al., 2011), temperate (Millar & Stephenson, 2015), and tropical rain forests (McDowell et al., 2018; Phillips et al., 2009). This is projected to have enormous impacts on the structure and function of forest ecosystems (Johnson et al., 2016), global biogeochemical cycles (Reichstein et al., 2013), and provisioning of ecosystem services (Anderegg, Kane, & Anderegg, 2012). Thus, understanding the mechanisms driving tree death during drought and which trees are most vulnerable is a high priority (Allen et al., 2010). Meta-analyses have shown that morphological (Greenwood et al., 2017) and/or hydraulic traits (Anderegg et al., 2016) provide insight into mechanisms of tree mortality during drought. However, whether strong trait-drought vulnerability relationships present in global meta-analyses are also present at a regional scale is not clear, as trait coordination among axes of the leaf economics spectrum may show strong patterns at coarse but not local scales (Messier, McGill, Enquist, & Lechowicz, 2017), because of intra-specific variation (Hulshof & Swenson, 2010) or trait plasticity (Anderegg et al., 2018). Moreover, additional knowledge gaps remain, including the degree to which mechanisms such as hydraulic failure and carbon starvation account for mortality during extreme drought (Sala, Piper, & Hoch, 2010), which traits underlie these mechanisms, whether species' biogeographic distribution patterns along rainfall gradients correlate with vulnerability (Esquivel-Muelbert et al., 2017), and if larger trees are more susceptible to death than smaller individuals as some studies report (Bennett, McDowell, Allen, & Anderson-Teixeira, 2015; Trugman et al., 2018) or if younger individuals in early successional environments are more vulnerable (Uriarte et al., 2016).

Part of this confusion stems from the fact that it has been difficult to determine which traits or species characteristics predict mortality during drought because of the lack of appropriate demographic and trait data collected simultaneously for a large number of tree species exposed to severe natural drought. This problem is especially acute when considering particularly diverse ecosystems such as tropical forests. Critical observations designed to study the effects of natural drought in diverse tropical systems are lacking due to the unlikelihood of predicting the location of a catastrophic drought years in advance. However, these are precisely the kind of data that are needed to understand how forests will respond to ongoing and future changes in tropical rainfall regimes (Feng, Porporato, & Rodriguez-Iturbe, 2013).

During 2015, a severe El Niño Southern Oscillation (ENSO) was associated with a substantial decrease in precipitation and an increase in daily temperature in the tropics (Burton, Rifai, & Malhi, 2018; Cooley et al., 2019). This abnormally strong drought caused major damage to forests in northwestern Costa Rica and in doing so provided the opportunity to investigate the functional characteristics associated with species drought vulnerability under an optimal design, i.e., during an extreme natural event that resulted in high tree mortality. Because many species in seasonally dry tropical forests are already adapted to periodic water shortages, it has been an open question whether these ecosystems will be vulnerable or resilient to changes in rainfall (Allen et al., 2017). Here, we combined long-term demographic records (pre- and post-drought) from forest monitoring plots, additional surveys of mortality for over 6,200 trees from 53 species, measurements of functional and hydraulic traits, and geographic models of tree species' hydrologic niches for regenerating seasonally dry tropical forest. Our goals were to quantify the impact of the severe 2015 ENSO event on tree mortality, and to discriminate among multiple potential variables to find those that best explained which trees and species succumbed to drought. Our study firmly suggests that many of these tropical forest species are indeed sensitive to extreme drought, and helps to guide future empirical and modeling work by revealing the patterns and mechanisms of mortality in a single forest using a remarkably rich dataset in an understudied ecosystem.

2 | MATERIALS AND METHODS

2.1 | Study sites

We conducted this study in the northwestern region of Costa Rica at Sector Santa Rosa (10.848N, 85.628W), which is part of Área de Conservación Guanacaste (ACG), and Palo Verde National Park (10.358N, 85.358W), part of Área de Conservación Arenal-Tempisque. Mean annual temperature is ~25°C. Vegetation includes mixtures of early, mid, and late successional tropical dry forest plant associations (Gillespie, Grijalva, & Farris, 2000), with a regional tree species pool of ~140 species from 45 families (Powers, Becknell, Irving, & Perez-Aviles, 2009). Plant communities at Santa Rosa include sites on low fertility soils dominated by a species of oak, *Quercus oleoides* Schltdl. & Cham. (Powers et al., 2009). Soils in the region are heterogeneous in texture, depth, and fertility (Powers et al., 2009), and include parent materials such as volcanic tuff (Leiva, Mata, Rocha, & Gutiérrez-Soto, 2009) or limestone (Hartshorn, 1983) that have low water holding capacity, which may exacerbate the effects of low rainfall on trees. Unfortunately, we do not have georeferenced tree locations or high resolution soil maps, so our mortality analyses cannot address edaphic factors.

Annual precipitation differs slightly between the sites, ranging from a 35 year mean of 1,708 mm in Santa Rosa to a 10 year mean of 1,691 mm at Palo Verde (O'Brien, Aviles, & Powers, 2018). Both sites experience a strong 5–6 month dry season that usually spans from late November to mid-May. The strong ENSO of 2015 coincided with the lowest reported annual rainfall at Santa Rosa (626 mm) in the existing 35 year record from local, manual gauges (Figure S1) and a 64 year record from global datasets (Cooley et al., 2019). The lowest annual rainfall on record for Palo Verde occurred during 2014

(953 mm). The effects of exceptionally low rainfall in 2015 may also have been exacerbated by the shortened rainy season in 2014 (Castro, Sanchez-Azofeifa, & Sato, 2018). While we used the simple metric of annual rainfall to quantify the magnitude of the drought attributed to the 2015 ENSO, other drought indices corroborate the severity of the 2015 ENSO for both forests (Methods S1; Figure S1).

2.2 | Mortality data

Our data came from three sources that differ in the minimum stem diameter sampled (Table S1; see Methods S1 for details on how the datasets were merged). First, we used data from eighteen 0.1 ha long-term monitoring plots to obtain plot-level estimates of annual mortality rates as the percentage of newly dead trees to the total number of trees censused from 2008 to 2017. These plots were established along gradients of edaphic variation and forest age, and share a common history of secondary forest succession following abandonment from grazing or agriculture, and are described in detail elsewhere (O'Brien et al., 2018; Waring, Adams, Branco, & Powers, 2016). Estimated forest ages in 2008 ranged from 6 to 61 years and there are six plots in the oak forest in Santa Rosa, and six plots each in diverse dry forest in Santa Rosa and Palo Verde. The total number of trees (≥10 cm diameter at breast height [DBH]) included in the long-term monitoring plot dataset ranged from 670 to 770 among census years. Second, we added observations of tree mortality in 2015 in eight 0.2 ha transects located in intermediate aged secondary to mature forest including both oak and more diverse forest communities in Santa Rosa. In these transects, we identified all trees >10 cm DBH, measured diameters, and noted tree status as alive or recently dead. Third, we used other plot or focal tree datasets from Santa Rosa including three 1.0 ha plots with twelve 0.1 ha nested subplots for small diameter stems, and repeated monthly surveys of 293 trees initially established along trails to monitor flower and fruit production and phenology of trees used by primates. This third data type allowed us to increase our observations of mortality during 2015 for a total sample of ~6,200 trees, and also permitted analyses of smaller sizes classes, as 2.0 cm DBH was the smallest stem recorded in this dataset. Of these three combined data sources for 2015, there were 53 species with between 26 and 623 individuals, for which we estimated species-specific 2015 mortality rates (Data Table S1; Table S1). Multi-stemmed trees were only counted as dead if all of the stems died. In 2016 we repeated our mortality census during the wet season in the 18 long-term monitoring plots to verify that trees that had apparently died in 2015 were indeed still dead and/or had not resprouted (we found no resprouters and only a few trees that appeared dead in 2015 but alive in 2016). Thus, we may have overestimated mortality rates in 2015, but only slightly. In practice, distinguishing recently dead trees from live, leafless trees or trees that had died over a year before our censuses was not difficult using criteria of the presence of small branches and twigs in recently dead trees, absence of damage to bark, etc. (Methods S1).

We acknowledge that drought can interact with other disturbance agents such as fire (Brando et al., 2014), insects like bark beetles (Stephenson, Das, Ampersee, Bulaon, & Yee, 2019), and or/fungal pathogens (Oliva, Stenlid, & Martínez-Vilalta, 2014) in causing tree mortality. Indeed, it is likely that the oak trees in our study area are suffering from some fungal pathogen (J. S. Powers, personal observation). However, due to the unanticipated strength of the 2015 ENSO drought and the large number of species we sampled, we were not able to explicitly quantify interactions between drought and additional mortality agents in this study.

2.3 | Morphological and chemical traits and successional status

Many studies suggest that commonly measured morphological traits are correlated with response to drought (Aleixo et al., 2019; Greenwood et al., 2017). We used species-specific mean trait values from previously published data that were collected from multiple trees per species located in this region (Powers & Tiffin, 2010). The traits we used in the correlation analysis included wood density (g/cm^3), specific leaf area (SLA in units of cm^2/g), foliar nitrogen (%), and foliar phosphorus (%). Trait data were available for 41 species out of 53. A quantitative index of 34 species' distributional preferences along gradients of forest age (i.e., successional status) was obtained from a previous study in this region (Werden, Becknell, & Powers, 2018). We extracted maximum observed DBH from the combined 2015 dataset described above or our extensive measurements of forest plots in this region described elsewhere (Becknell & Powers, 2014) and used whichever of these values was largest.

2.4 | Hydraulic traits

We selected a subset of 18–20 species that spanned a range of mortality during the drought for further study (Data Table S1). These diverse species come from 14 families but also include four species from the Fabaceae, which is the most abundant and diverse family in the study region (Powers et al., 2009), and represent a range of leaf habits (e.g., evergreen, semideciduous and deciduous). We collected field data or collated values from previous studies members of our team have published (Brodribb, Holbrook, Edwards, & Gutierrez, 2003) for two hydraulic traits: turgor loss point (TLP) and leaf P_{50}, i.e., water potential at 50% leaf xylem embolism. TLP was obtained by constructing pressure–volume curves (PV-curves; Tyree & Hammel, 1972). To sample plant material for the PV-curves we collected >1 m long canopy branches during predawn and returned them to the lab inside black plastic bags where we selected fully expanded new leaves that were cut under water and allowed to hydrate completely for 2–3 hr, ensuring an initial water potential close to zero. Leaves were then allowed to dehydrate while periodically measuring water potential and leaf mass. To obtain TLP from the PV-curves we estimated the saturated

water content (SWC, g) of a leaf and then calculated the relative water content as RWC = (H_2O_{mass}/SWC) × 100. We regressed the inverse leaf water potential against 100-RWC to obtain TLP as the value when the slope changes (Bartlett, Scoffoni, & Sack, 2012; Tyree & Hammel, 1972). For many of the species, multiple TLP measurements were made by one to three different observers over time and averaged.

Leaf water potential at 50% embolism (leaf P_{50}) was measured using the optical method to visually quantify the number of embolism events in leaf veins (Brodribb et al., 2016). Although this technique indicates the area of cavitation in the leaf, it has been shown to closely reflect changes in hydraulic resistance (Brodribb et al., 2016). Measurements were made on two to three adult trees per species and averaged. We collected sun exposed branches >1 m long before dawn to ensure maximum leaf water potentials and minimal tension on the water column, after cutting samples down they were transported immediately to the field station in bags. We measured water potentials on two leaves per sample, before the start of the embolism quantification to ensure water potentials >−0.5 MPa. We did not measure vessel length in this study; however, in a different study at this site, we measured vessel lengths for a large number of many of the same species, and they ranged from 14.1 to 70.5 cm, with a mean value of 36.3 cm (G. Vargas G., unpublished data). A psychrometer (ICT) was fitted to the distal part of branches and a mature leaf was enclosed in an Epson Perfection V800 Photo Color Scanner (Epson America, Inc.) that took high resolution images of the leaves dehydrating while attached to their respective branches. Leaves were scanned every 5 min as branches dehydrated, and the appearance of embolisms in the leaf vasculature was quantified by image analysis (see www.opensourceov.org for details). Initially, we made sporadic measurement of water potential with a pressure chamber to ensure consistency between the psychrometers and pressure chamber and verify that the psychrometers were installed correctly. Leaves were considered 100% embolized when no more embolisms were observed for a period of 5 hr and they appeared crispy dry. Plots of water potential versus cumulative embolism were used to determine the water potential at 50% embolism (leaf P_{50}). In these cases, we used average values per species. For both leaf P_{50} and TLP, we collected branches from apparently healthy mature trees in ACG (Sectors Santa Rosa and Horizontes) during the months of early July to late October which represent the wettest period of the year.

We were interested in the "hydraulic safety margin" of trees (HSM), which measured the extent to which plants protect their water transport systems from damage associated with xylem embolism. Other studies have previously defined HSM based upon stem traits as the difference between the minimum water potential (Ψ_{min}) and water potential at 50% loss of conductivity (Ψ_{50}; Choat et al., 2012). However, in our study system previous work has shown that tree water loss is greatly reduced when leaf water potential approaches the TLP triggering stomatal closure (Brodribb & Holbrook, 2003) and likely leaf shedding (Wolfe, Sperry, & Kursar, 2016). Thus we defined the HSM based on leaf measurements as the difference between leaf P_{50} and TLP for a species. Trees that shut their stomata far in advance of the water potential at which they reach 50% leaf embolism have a larger stomatal safety margin and should be able to avoid damaging xylem embolism for longer than species with a smaller difference between leaf P_{50} and TLP (Brodribb & Holbrook, 2004). To avoid confusion, we refer to our measurement of leaf water potential at 50% loss of conductance as leaf P_{50} throughout the text.

2.5 | Hydrologic niches

We accessed georeferenced occurrence records for all species in our dataset from the BIEN database (http://bien.nceas.ucsb.edu/bien/). Two species did not appear in this database (*Cedrela odorata* and *Simarouba glauca*). In those cases we used occurrence records from Global Biodiversity Information Facility (GBIF; www.gbif.org). There were three species that we could not obtain information for, in two cases because we only had species identifications to genus and in one case because there were no records in either BIEN or GBIF. We extracted average monthly rainfall (from years 1979 to 2013) for each record from the Climatologies at High Resolution for the Earth's Land Surface Areas (CHELSA) dataset (Karger et al., 2017), which has a spatial resolution of 30 arc-seconds. With these mean monthly rainfall climatologies we calculated annual rainfall and the seasonality index (Feng et al., 2013), a measure of rainfall seasonality that incorporates the magnitude of rainfall and the concentration of that rainfall in the wet season, and dry season length (i.e., number of months with climatic water deficit <0) for each occurrence record. Annual rainfall, seasonality index, and dry season length values were averaged across occurrence records for each species to define the hydrological niche. If there was more than one species occurrence record within one CHELSA cell, that cell was only counted once in calculating summary statistics. The number of CHELSA cells that went into the niche models ranged from 5 to 5,495 with an average of 992 grid cells per species.

2.6 | Statistical analyses

Our first question was whether plot-level mortality rates differed significantly among years from 2009 to 2017 in the 18 long-term monitoring plots. For this analysis, we counted the number of dead trees per year and the total number of trees, including all stems ≥10 cm DBH for each of the 18 plots and used a bootstrapped Fisher exact test with 10,000 samples. *p*-Values were estimated using a Monte Carlo simulation procedure to test whether the ratio of dead trees to total trees was independent of year (p = .00001). Furthermore, we performed a bootstrap test with 10,000 samples to see whether for each year mortality rate *z*-values were different from "background" mortality rate *z*-value (i.e., defining background mortality as the 9 year mean mortality rate for all years). To perform this analysis, we calculated *z*-values as follows:

$$z_{iy} = \left(r_i - \bar{r}_b\right) / \overline{\sigma}_b,$$

where for a given plot i at a given year y the z value could be described as the mortality rate r minus the bootstrapped background

mortality rate estimated as the global mean mortality rate for all the plots in all years ($\bar{r}_b$) divided by the standard deviation ($\bar{\sigma}_b$) of $\bar{r}_b$. Then the probability of mortality being higher (p_y) for a given year was calculated as:

$$p_y = \frac{\sum_{z_{iy} \leq z_b} z_{iy}}{n},$$

where z_{iy} represents the z value for each bootstrapped plot i at a given year y, z_b the background mortality rate z-value, and n the total number of bootstrapped samples. With this approach we were able to corroborate that mortality rates during 2015 and 2016 were significantly higher than the background mortality rates (Table S2). We performed additional analyses to rule out the possibility that elevated plot-level mortality rates were due to a single, exceptionally vulnerable species (Figure S2).

Second, we investigated the role of tree diameter in determining mortality patterns. We first compared the diameters of trees that died during 2015 to trees that died during other years using an unpaired Wilcoxon test using the 18 long-term plot data (Figure S3). Next, to better understand whether size helped to explain which trees died during 2015 in the combined 2015 dataset, we performed a logistic regression with mortality as a binary response variable (0 = alive in 2015, 1 = died in 2015) for all the pooled individuals from all transects (stems ≥ 10 cm DBH) and plots (stems ≥ 2.2 cm DBH). We used individual trees' DBH as our metric of tree size, and we used the value for the single stem with the largest diameter for multi-stemmed trees. Analyses were restricted to the 53 species with ≥26 individuals. We performed two analyses. The first model did not include species as an effect. In this model, the probability of mortality is described by:

$$\text{Mortality}_i \sim B(1, \pi_i),$$

$$E(\text{Mortality}_i) = \pi_i \quad \text{and} \quad \text{var}(\text{Mortality}_i) = \pi_i \times (1 - \pi_i),$$

$$\log(\pi_i/(1-\pi_i)) = \alpha + \beta \times \text{DBH}_i.$$

In this logistic regression model, Mortality_i is binomial distributed with probability π_i and n_i = 1 independent trials (one tree can only die once). The log odds ratio of π_i is described as a linear response to DBH_i. With this approach we found a significant effect of DBH_i on mortality rates (α = −3.0400, β = 0.0094, p = .0111), implying a slight increase in the probability of mortality (π_i) toward larger DBH_i values. Pr(Dead|DBH) values ranged from 0.04 in smaller size classes to 0.2 in larger size classes, which follows right skewed tree size distribution in the community.

We also investigated whether mortality risk and its dependence on size varied among species. In this model, the probability of mortality is described by:

$$\text{Mortality}_i|\text{Species}_i \sim B(1, \pi_i),$$

$$E(\text{Mortality}_i) = \pi_i \quad \text{and} \quad \text{var}(\text{Mortality}_i) = \pi_i \times (1 - \pi_i),$$

$$\log(\pi_i/(1-\pi_i)|\text{Species}_i) = \alpha + \text{Sp}_{0i} + \beta \times \text{DBH}_i,$$

$$\text{Sp}_{0i} \sim N(0, \tau^2).$$

Similar to the first model, in this logistic regression model, $\text{Mortality}_i|\text{Species}_i$ is binomial distributed with probability π_i and n_i = 1 independent trials. The log odds ratio of π_i for any given species is described as a linear response to DBH_i. When including species in the model, the significant effect of DBH_i on mortality rates disappeared (α = −2.7560, Sp = 0.8793, β = 0.0055, p = .0692), suggesting that the dependence of mortality on tree size varies among species. To test for this possibility, we performed species-specific logistic regressions for each of the 53 abundant species in the combined 2015 dataset (Data Table S1). Full details of these analyses and goodness-of-fit tests appear in Methods S1.

Our next question was whether traits (morphological, chemical, or hydraulic), maximum tree size, successional status or dimensions of species' hydrologic niches were correlated with species-specific 2015 mortality rates estimated from the full dataset. For this, we used Pearson weighted correlation coefficients with each species as a data point weighted by sample size, i.e., number of individuals, used to estimate 2015 mortality rates, for all analyses involving mortality. The rationale for weighting 2015 mortality rates by sample size is that our confidence in the mortality estimates is higher for species represented by a larger number of individuals.

We performed a bootstrapped estimation of the standard errors for each correlation using 5,000 samples, in order to address heteroscedasticity in the correlations and to obtain more reliable p values. For the pairwise correlations among all variables that excluded 2015 mortality rates, we used the same bootstrap approach but without any weighting. The number of species differed among analyses because we did not have measurements of all traits for all species. Variables included in this analysis were: 2015 mortality rate, leaf P_{50}, TLP, HSM (TLP-leaf P_{50}), wood density, specific leaf area, foliar phosphorous, foliar nitrogen, maximum DBH, mean rainfall niche, mean rainfall seasonality, dry season length, and successional status. We also investigated whether species-specific mortality rates during the drought or traits differed among leaf phenology groups (i.e., evergreen, deciduous, and semideciduous species) using a Kruskal–Wallis rank sum test for mortality rates, and analysis of variance (ANOVA) for the other traits.

We then used regression analysis to determine the relationship between species-specific mortality rates during the drought and the best correlated variables, HSM and mean seasonality, to determine whether these relationships are linear or otherwise. We fit four models to the relationship between mortality and HSM or seasonality index (linear, quadratic polynomial, quadratic splines and piecewise regression). Confidence intervals for each model were generated through 5,000 bootstrapped samples to generate confidence intervals and we used the Akaike information criterion (AIC) to select the model that best fit the data (Tables S2 and S3). All analyses were conducted in the R 3.2.3 statistical software (R Core Team, 2017), using packages car (Fox & Weisberg, 2011), Hmisc (Harrell Jr & Dupont, 2018), lme4 (Bates, Maechler, Bolker, & Walker, 2015),

mass (Venables & Ripley, 2002), segmented (Muggeo, 2003, 2008), and splines (R Core Team, 2017).

3 | RESULTS

Predrought average annual mortality rates among trees in all plots ranged from a low of 0.66% to a high of 3.08% during 2009–2014 (Figure 1). By contrast, the mortality rate in these same plots during the extreme drought of 2015 increased significantly to 6.14% and remained elevated in 2016, before returning to more typical, lower rates in 2017 (Figure 1; Table S1). We ruled out the possibility that these plot-level mortality patterns were biased by a single dominant species that was extremely vulnerable to low rainfall by comparing average, background mortality rates (2009–2014) to 2015 mortality rates for 23 abundant species in these plots with a Wilcoxon signed rank test (W = 115, p = .008; Figure S2). The fact that the year with the highest mortality rates at both the plot- and species-level coincided with the strong ENSO event clearly suggests a causal link between tree mortality and low rainfall.

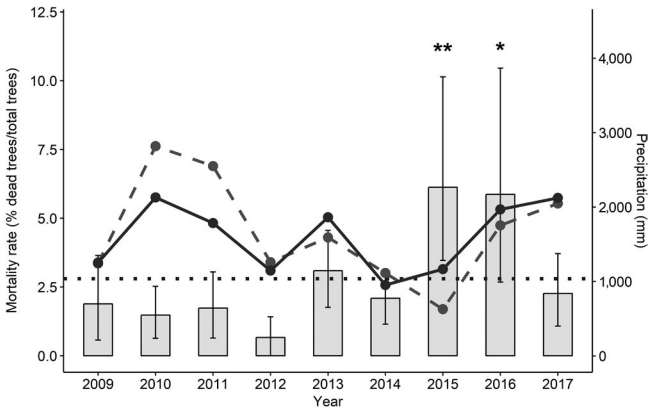

FIGURE 1 Yearly precipitation in Sector Santa Rosa in the Área de Conservación Guanacaste (dashed line) and Parque Nacional Palo Verde, Costa Rica (continuous line) and annual plot-level mortality rates of trees ≥10 cm diameter at breast height in 18 0.1 ha long-term monitoring plots (12 plots in Santa Rosa and six plots in Palo Verde) from 2009 to 2017. Error bars represent the 97.5% confidence intervals from a bootstrap with 10,000 samples. Significance levels (*p < .05 and **p < .01) represent the probability that the bootstrapped mean mortality for a given year is greater than the bootstrapped mean mortality over the 9 year period of background mortality rates (dotted line). Data were pooled between the two conservation areas for analysis to yield more robust estimates of interannual variation in mortality rates

In our expanded dataset from 2015, there were 53 tree and shrub species with between 26 and 623 individuals per species for which we calculated species-specific ENSO-mortality rates as the percentage of individuals that died during 2015. Overall, species-specific mortality rates during the 2015 ENSO varied enormously, from a low of 0% to a high of 34% (Figure 2). Mortality rates did not vary consistently among species with different leaf habits (Kruskal–Wallis χ^2 = 1.23, df = 2, p = .5277; Figure S4).

Compared to diameters of trees that died in previous years in the 18 forest inventory plots (which only censuses trees ≥10 cm DBH), the average diameter of trees that died in 2015 (12.8 cm) was smaller than that of trees that died outside of the drought year (16.9 cm; W = 9,063.5, p = 0.0019; Figure S3). We further examined the relationship between diameter and probability of mortality during drought in the expanded 2015 dataset. Consistent with some other studies (Phillips et al., 2010), the relationship between mortality rate and size (as indexed by DBH) depended on species (Figure 3). Of the 53 species we studied, only five had significant relationships (p < .05) between tree size as indexed by diameter and probability of dying during the 2015 drought (Figure 3; Data Table S1). Of these

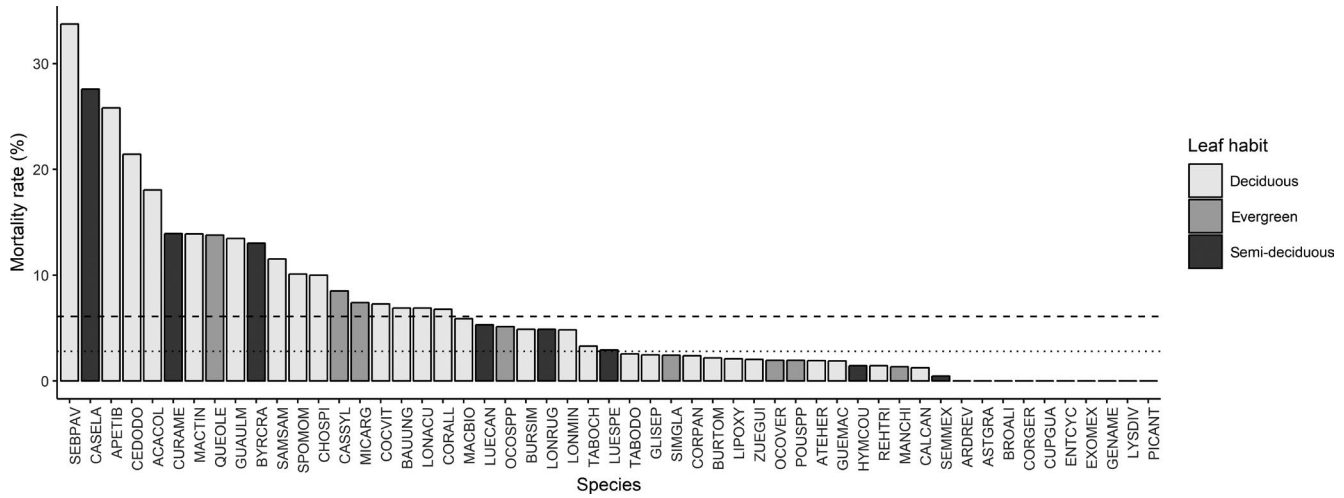

FIGURE 2 Species-specific mortality rates during an extreme drought for 53 species in seasonally dry tropical forest in northwestern Costa Rica using the combined dataset of trees sampled in 2015 only. The dotted line represents average plot-level mortality rates from 2009–2014 in 18 long-term forest plots (trees >10 cm diameter at breast height) and the dashed line indicates the average plot-level mortality rate during the 2015 El Niño Southern Oscillation derived from the same plots. Refer to Data Table S1 for species codes. Species are color-coded by leaf phenology (i.e., evergreen, deciduous, or semideciduous)

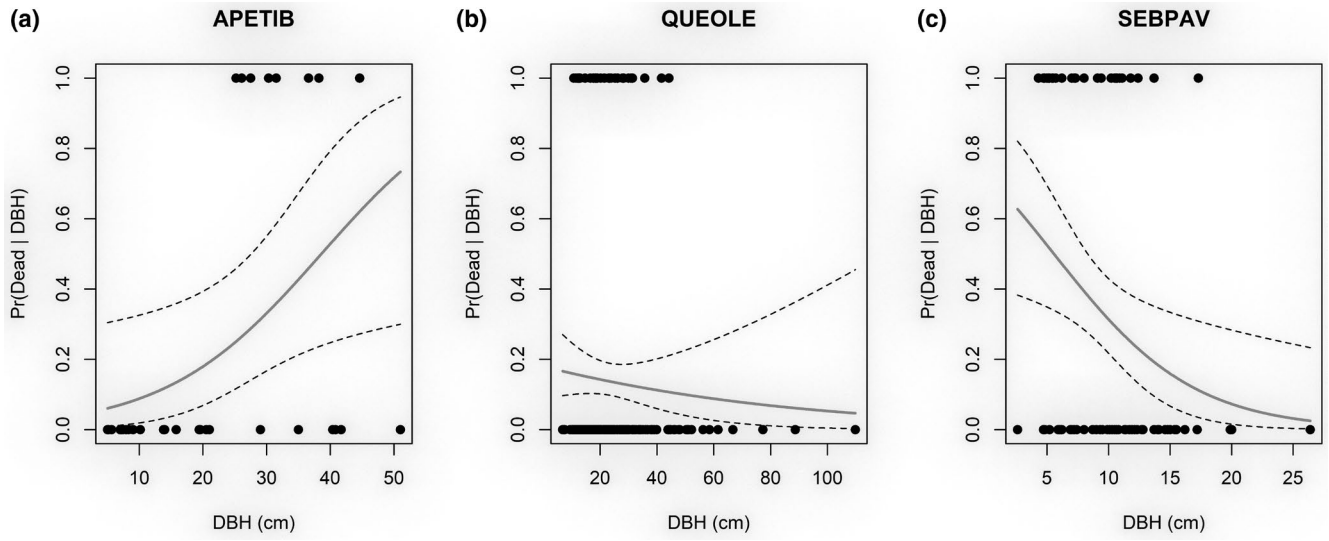

FIGURE 3 Mortality during the 2015 El Niño Southern Oscillation as a function of diameter at breast height for three species showing contrasting patterns, (a) *Apeiba tibourbou* (increasing), (b) *Quercus oleoides* (no relationship), and (c) *Sebastiana pavoniana* (decreasing). Analyses were based on the 2015 combined dataset. DBH, diameter at breast height

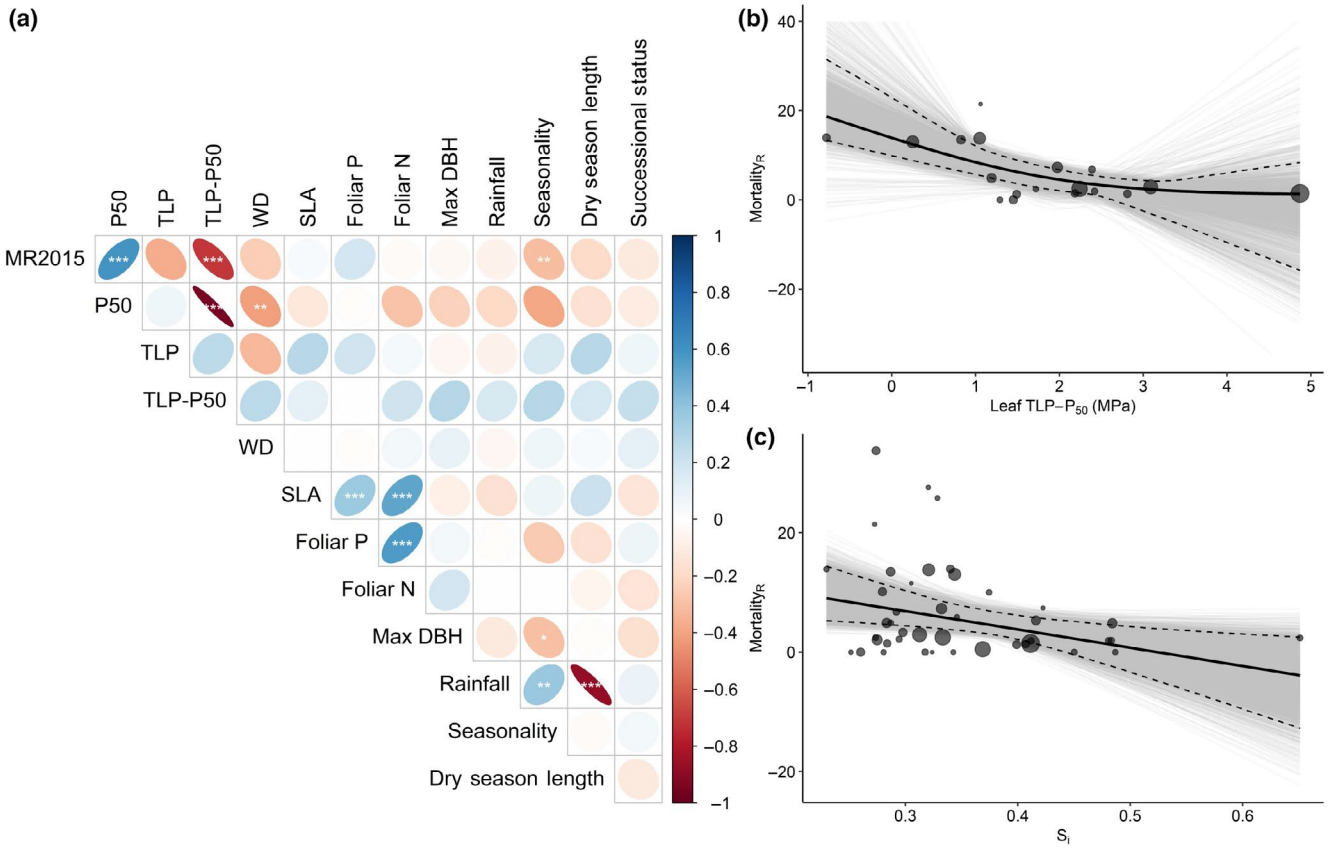

FIGURE 4 (a) Pearson correlation coefficients for pairwise relationships among species-specific 2015 mortality rates from the combined dataset (MR2015), traits, hydrologic niches (mean annual rainfall, seasonality, and dry season length) and an index of successional status. The number of species used in each analysis was 18–19 for all correlations involving hydraulic traits, but otherwise varied depending upon available data. See Supporting Information for full details. Significance levels at: $p < .05$ (*), $p < .01$ (**) and $p < .001$ (***) are indicated as white asterisks within cells in the correlation matrix. (b) Bootstrapped regression models of tree mortality rates during the 2015 El Niño Southern Oscillation are related to hydraulic safety margin, as measured by turgor loss point minus leaf P_{50} ($R^2 = .62$, $p = .0007$) and (c) and seasonality index ($R^2 = .09$, $p = .0488$). Where each point represents one species, point sizes according to sample size (min = 26; max = 623), black lines represent the bootstrapped mean estimate of mortality for a given value of each predictor, dashed lines represent 95% bootstrapped confidence intervals, and gray lines represent each of the 5,000 bootstrapped mean estimates of mortality for a given value of each predictor

species, three showed increasing probability of mortality with size and two showed decreasing probabilities as size increased (Data Table S1). Sample sizes used to estimate mortality rates are unlikely to have played a role in these results because they ranged from 29 to 423 for the group of species with significant size relationships, and from 26 to 623 for the rest of the species.

The weak relationships between tree size and mortality at our field sites suggest that other factors such as interspecific differences in species' functional characteristics may play an important role in response to drought. Despite marked interspecific variation in traits and distribution characteristics (Data Table S1), only three variables were significantly correlated with species-specific 2015 mortality rates (Figure 4a): leaf P_{50} (r = .60; p = .00001), HSM (r = −.70; p = .00001; Figure 4b) and mean rainfall seasonality niche (r = −.31; p = .002; Figure 4c). These results were qualitatively consistent whether correlations were weighted by species sample size or not (results not shown). Species that had large HSMs experienced little to no mortality during the extreme drought, while trees with narrow HSMs had high mortality rates (Figure 4a,b). The fact that neither maximum diameter nor successional status was correlated with mortality rates in any analysis suggests that our results are not biased by the inclusion of species from early successional groups or species that are small statured. Further analysis revealed a non-linear relationship as the best fit between mortality and HSM (Table S2) and a linear relationship for mean seasonality niche (Table S3). Last, it is unlikely that the strong relationship between HSM and mortality during the drought was mediated by leaf habit or leaf phenology, as all traits except for foliar nitrogen did not vary consistently among deciduous, evergreen, or semideciduous species (Figure S5).

4 | DISCUSSION

There is widespread interest in understanding when and where trees die in response to drought (Allen et al., 2010). In species-rich ecosystems such as tropical forests, high diversity further hampers our ability to understand vulnerability to extreme climate events. Our long-term demographic data and large databases of functional and hydraulic traits, coupled with the extreme natural drought event in 2015 that resulted in high tree mortality, provided an unprecedented opportunity to understand the functional characteristics that underlie variation in tree responses. Prior meta-analyses have established links between hydraulic traits and mortality (Anderegg et al., 2016; Griffin-Nolan et al., 2018), and other studies have shown links between hydraulic traits and other metrics of forest performance such as canopy conductance (Barros et al., 2019) or sap flux (Maréchaux et al., 2018). By contrast, our results are novel in that they demonstrate a strong relationship between hydraulic traits and mortality for a large number of co-occurring species, which is perhaps the most extreme potential response to drought.

Thus, our results provide strong, albeit indirect, evidence that hydraulic failure is the causal mechanism of tree mortality during extreme drought in northwestern Costa Rica. We tamper this conclusion by acknowledging that HSM was the best predictor of mortality among the variables that we measured; there may be other important traits we did not measure that may contribute to drought resistance. Nevertheless, in our study system tree species with large safety margins apparently avoided lethal damage to their vascular systems either by closing stomata early in drought or by producing embolism-resistant xylem. This damage avoidance strategy appears to outweigh other potential adaptive strategies such as leaf phenology (which was not correlated with mortality; Figure S4) or rooting depth, which does vary as a function of leaf habit (Smith-Martin, Xu, Medvigy, Schnitzer, & Powers, 2019), suggesting that hydraulic safety is the primary determinant of mortality during drought (Martin-St Paul, Delzon, & Cochard, 2017). The association between HSM, which in this case was a foliar index, and tree mortality emphasizes the integrative capacity of the leaf in terms of registering and responding to whole-plant stress. This result suggests that there is little systematic variation in xylem vulnerability to embolism between tissues within an individual plant, or that variation scales with the sensitivity of the leaf to embolism. Recent studies across diverse species support this explanation suggesting that root, stem and leaf tissues within individual plants are relatively coordinated in their vulnerability to embolism (Rodriguez-Dominguez, Carins Murphy, Lucani, & Brodribb, 2018; Skelton, Brodribb, & Choat, 2017).

Tree survial during drought depends on a number of factors including cambial vitality, which in turn may depend on various other traits, such as bark/stem transpiration, hydraulic capacitance (of bark and xylem tissue), and compartmentalization. Nevertheless, our data contribute to the growing evidence for an association between the vulnerability of plant hydraulic systems to embolism and the prospects of plants incurring damage during drought (Choat et al., 2018). By combining detailed tree survey data with targeted hydraulic characterization of species during a major tropical die-back event our study provides strong support for the use of embolism thresholds and plant safety margins as predictive metrics for understanding drought mortality. The advantage of such metrics is that they can be used to parameterize mechanistic models of plant gas exchange (Sperry et al., 2016) and survival (Martin-St Paul et al., 2017), thus providing the potential to predict not only productivity, but also community structure under future climatic scenarios. Importantly, traits such as wood density, SLA, and foliar nutrients were poorly correlated with vulnerability to drought or hydraulic traits (Figure 4a). This casts doubt about the utility of the so-called "leaf economics spectrum" or morphological traits to predict vulnerability to drought, as some meta-analyses (Greenwood et al., 2017) and other long-term demographic studies suggest (Aleixo et al., 2019), and identifies hydraulic traits as high priorities for further study. Our results also highlight a role for geographic distribution data in forecasting which species are vulnerable to drought in particular regions (Figure 4c; Esquivel-Muelbert et al., 2017). In our local study region with a very seasonal rainfall distribution, tree species whose core distributions are in areas that experience less

seasonal rainfall suffered the most mortality during this extreme event.

While our results provide strong evidence of linkages between vulnerability to drought and HSMs, our analyses provided surprisingly little support for any relationship—positive or negative—between mortality and tree size. Many studies have found that larger trees are more vulnerable to drought than smaller ones (Bennett et al., 2015; Trugman et al., 2018), while others have predicted that younger and presumably smaller trees have higher drought-induced mortality in secondary forest landscapes (Uriarte et al., 2016). Our study landscape is dominated by secondary forests (typically >20–40 years after the removal of agriculture and grazing; Calvo-Alvarado, McLennan, Sanchez-Azofeifa, & Garvin, 2009), which initially led us to expect higher mortality in smaller size classes. However, it appears that tree size is not an important predictor of mortality during extreme drought for the majority of species in this forest. It is possible that species-specific hydraulic traits that underpin vulnerability to drought supersede tree size or successional status of the species in this regenerating forest. Similarly, in a study of the interactions between bark beetles and tree mortality during a severe drought in the Sierra Nevada mountains of California, tree species-specific bark beetles attacked different size classes of trees, which effectively precluded any general relationship between tree size and vulnerability to drought (Stephenson et al., 2019). Thus, species-specific information may be required to predict the demographic impacts of drought-induced mortality.

Last, although we were limited in our ability to explore fully legacy effects of drought, the data from our long-term plots do indeed suggest such effects. Mortality rates continued to be elevated above background rates in 2016, even though rainfall rebounded (Figure 1). This is consistent with light detection and ranging (LiDAR)-based observations of declining forest biomass in the Amazon three to four years after a severe drought (Yang et al., 2018) and declines in growth rates inferred from tree rings in Northern Hemisphere forests (Anderegg et al., 2015). Whether the same mechanism, i.e., hydraulic failure, or other explanations such as carbon starvation are responsible for the lagged mortality following extreme drought in the dry forest we studied in Costa Rica deserves further study.

Drought has well-documented effects on tropical moist and wet forest carbon cycling (Phillips et al., 2009) and species composition (Condit, 1998). Here we show that regenerating, seasonally dry tropical forest is similarly sensitive to changes in rainfall and an extreme drought. Determining whether these patterns are generalizable to other tropical dry and wet forests is an important question, but one that will likely be hampered by the lack of appropriate data for other sites. In our study sites, through the availability of long-term demographic data, extensive databases of functional and hydraulic traits for these species collected in this same region (Powers & Tiffin, 2010) and assessments of hydrologic niches, we were able to identify the most important correlates of tree responses to drought. Our data thus fill a critical gap in understanding forest mortality. While previous studies highlight the importance of hydraulic failure in artificially imposed drought (Rowland et al., 2015), or by global meta-analysis (Anderegg et al., 2016), we present data from perhaps the most informative of all experimental scenarios: a natural, diverse tropical forest system under natural drought. Benefitting from the fortuitous occurrence of a major El Niño in 2015 and the co-occurrence of complementary long-term research projects facilitated by research policy in the ACG, we were able to clearly identify HSM as the best predictor of interspecific variation in mortality during a natural extreme drought event. Importantly, this is exactly the type of drought event that is predicted to become more frequent in the future across the entire Pacific region. Thus, our results carry clear implications for conservation, restoration, forestry, and land management in this region. As tropical climates become more variable (Feng et al., 2013) and droughts increase in severity, seasonally dry forest landscapes and the current tree species they support will likely change, which may compromise both biodiversity conservation and the capacity of these forests to store carbon. Understanding the hydraulic properties of tree species will provide a means of predicting changes in forest structure, improving simulation models of forest dynamics, as well as identifying species under threat.

ACKNOWLEDGEMENTS

We thank the following funding sources for making this work possible: the United States National Science Foundation CAREER grant DEB 1053237, NSF PRFB 1711366, NSF Inter-American Institute for Global Change Research (IAI) CRN3025, grant number GrantGEO-128040, the Technological Institute of Costa Rica, ARC DP170100761, Chester Zoo (United Kingdom), National Geographic Society, Consejo Nacional por la Ciencia y la Tecnología (CONACyT, Mexico), and the US Department of Energy, Office of Science, Office of Biological and Environmental Research, Terrestrial Ecosystem Science (TES) Program (award number DESC0014363).

AUTHOR CONTRIBUTION

J.S.P., G.V.G., T.J.B., and D.M. conceptualized the project with input from R.B. and N.B.S. D.P., J.M.B., C.M.S., F.A., E.C., A.J.C., M.M.C., D.C., C.D.J., E.M.C., and L.K.W. collected the data. G.V.G., J.S.P., N.B.S., and J.C.C. analyzed the data with input from X.X. J.S.P. wrote the manuscript with input from G.V.G., T.J.B., and D.M. All co-authors contributed to edits.

DATA AVAILABILITY STATEMENT

Summaries of functional trait data grouped by species appear in online Table S1. Mortality data for the 18 plot long-term dataset and the 2015 combined dataset, along with R scripts for data analysis, are available from the Dryad Digital Repository at the following https://doi.org/10.5061/dryad.2rbnzs7jp

ORCID

Jennifer S. Powers https://orcid.org/0000-0003-3451-4803
Xiangtao Xu https://orcid.org/0000-0002-9402-9474
David Medvigy https://orcid.org/0000-0002-3076-3071

REFERENCES

Aleixo, I., Norris, D., Hemerik, L., Barbosa, A., Prata, E., Costa, F., & Poorter, L. (2019). Amazonian rainforest tree mortality driven by climate and functional traits. *Nature Climate Change*, *9*(5), 384–388. https://doi.org/10.1038/s41558-019-0458-0

Allen, C. D., Macalady, A. K., Chenchouni, H., Bachelet, D., McDowell, N., Vennetier, M., … Cobb, N. (2010). A global overview of drought and heat-induced tree mortality reveals emerging climate change risks for forests. *Forest Ecology and Management*, *259*(4), 660–684. https://doi.org/10.1016/j.foreco.2009.09.001

Allen, K., Dupuy, J. M., Gei, M. G., Hulshof, C. M., Medvigy, D., Pizano, C., … Powers, J. S. (2017). Will seasonally dry tropical forests be sensitive or resistant to future changes in rainfall regimes? *Environmental Research Letters*, *12*, 023001. https://doi.org/10.1088/1748-9326/aa5968

Anderegg, L. D. L., Berner, L. T., Badgley, G., Sethi, M. L., Law, B. E., & HilleRisLambers, J. (2018). Within-species patterns challenge our understanding of the leaf economics spectrum. *Ecology Letters*, *21*, 734–744. https://doi.org/10.1111/ele.12945

Anderegg, W. R. L., Kane, J. M., & Anderegg, L. D. L. (2012). Consequences of widespread tree mortality triggered by drought and temperature stress. *Nature Climate Change*, *3*, 30–36. https://doi.org/10.1038/nclimate1635

Anderegg, W. R. L., Klein, T., Bartlett, M., Sack, L., Pellegrini, A. F. A., Choat, B., & Jansen, S. (2016). Meta-analysis reveals that hydraulic traits explain cross-species patterns of drought-induced tree mortality across the globe. *Proceedings of the National Academy of Sciences of the United States of America*, *113*(18), 5024–5029. https://doi.org/10.1073/pnas.1525678113

Anderegg, W. R. L., Schwalm, C., Biondi, F., Camarero, J. J., Koch, G., Litvak, M., … Pacala, S. (2015). Pervasive drought legacies in forest ecosystems and their implications for carbon cycle models. *Science*, *349*, 528–532. https://doi.org/10.1126/science.aab1833

Barros, F. D. V., Bittencourt, P. R. L., Brum, M., Restrepo-Coupe, N., Pereira, L., Teodoro, G. S., … Oliveira, R. S. (2019). Hydraulic traits explain differential responses of Amazonian forests to the 2015 El Niño-induced drought. *New Phytologist*, *223*(3), 1253–1266. https://doi.org/10.1111/nph.15909

Bartlett, M. K., Scoffoni, C., & Sack, L. (2012). The determinants of leaf turgor loss point and prediction of drought tolerance of species and biomes: A global meta-analysis. *Ecology Letters*, *15*, 393–405. https://doi.org/10.1111/j.1461-0248.2012.01751.x

Bates, D., Maechler, M., Bolker, B., & Walker, S. (2015). Fitting linear mixed-effects models using lme4. *Journal of Statistical Software*, *67*, 1–48. https://doi.org/10.18637/jss.v067.i01

Becknell, J. M., & Powers, J. S. (2014). Stand age and soils as drivers of plant functional traits and aboveground biomass in secondary tropical dry forest. *Canadian Journal of Forest Research*, *44*, 603–614. https://doi.org/10.1139/cjfr-2013-0331

Bennett, A. C., McDowell, N. G., Allen, C. D., & Anderson-Teixeira, K. J. (2015). Larger trees suffer most during drought in forests worldwide. *Nature Plants*, *1*(10). https://doi.org/10.1038/nplants.2015.139

Brando, P. M., Balch, J. K., Nepstad, D. C., Morton, D. C., Putz, F. E., Coe, M. T., … Soares, B. S. (2014). Abrupt increases in Amazonian tree mortality due to drought-fire interactions. *Proceedings of the National Academy of Sciences of the United States of America*, *111*, 6347–6352. https://doi.org/10.1073/pnas.1305499111

Brodribb, T. J., & Holbrook, N. M. (2003). Stomatal closure during leaf dehydration, correlation with other leaf physiological traits. *Plant Physiology*, *132*(4), 2166–2173. https://doi.org/10.1104/pp.103.023879

Brodribb, T. J., & Holbrook, N. M. (2004). Stomatal protection against hydraulic failure: A comparison of coexisting ferns and angiosperms. *New Phytologist*, *162*(3), 663–670. https://doi.org/10.1111/j.1469-8137.2004.01060.x

Brodribb, T. J., Holbrook, N. M., Edwards, E. J., & Gutierrez, M. V. (2003). Relations between stomatal closure, leaf turgor and xylem vulnerability in eight tropical dry forest trees. *Plant, Cell and Environment*, *26*(3), 443–450. https://doi.org/10.1046/j.1365-3040.2003.00975.x

Brodribb, T. J., Skelton, R. P., McAdam, S. A. M., Bienaime, D., Lucani, C. J., & Marmottant, P. (2016). Visual quantification of embolism reveals leaf vulnerability to hydraulic failure. *New Phytologist*, *209*(4), 1403–1409. https://doi.org/10.1111/nph.13846

Burton, C., Rifai, S., & Malhi, Y. (2018). Inter-comparison and assessment of gridded climate products over tropical forests during the 2015/2016 El Nino. *Philosophical Transactions of the Royal Society B: Biological Sciences*, *373*(1760), 10. https://doi.org/10.1098/rstb.2017.0406

Calvo-Alvarado, J., McLennan, B., Sanchez-Azofeifa, A., & Garvin, T. (2009). Deforestation and forest restoration in Guanacaste, Costa Rica: Putting conservation policies in context. *Forest Ecology and Management*, *258*, 931–940. https://doi.org/10.1016/j.foreco.2008.10.035

Castro, S. M., Sanchez-Azofeifa, G. A., & Sato, H. (2018). Effect of drought on productivity in a Costa Rican tropical dry forest. *Environmental Research Letters*, *13*(4), 045001. https://doi.org/10.1088/1748-9326/aaacbc

Choat, B., Brodribb, T. J., Brodersen, C. R., Duursma, R. A., López, R., & Medlyn, B. E. (2018). Triggers of tree mortality under drought. *Nature*, *558*(7711), 531–539. https://doi.org/10.1038/s41586-018-0240-x

Choat, B., Jansen, S., Brodribb, T. J., Cochard, H., Delzon, S., Bhaskar, R., … Zanne, A. E. (2012). Global convergence in the vulnerability of forests to drought. *Nature*, *491*, 752–755. https://doi.org/10.1038/nature11688

Condit, R. (1998). Ecological implications of changes in drought: Shifts in forest composition in Panama. *Climatic Change*, *39*, 413–427. https://doi.org/10.1023/A:1005395806800

Cooley, S. S., Williams, C. A., Fisher, J. B., Halverson, G. H., Perret, J., & Lee, C. M. (2019). Assessing regional drought impacts on vegetation and evapotranspiration: A case study in Guanacaste, Costa Rica. *Ecological Applications*, *29*(2), e01834. https://doi.org/10.1002/eap.1834

Esquivel-Muelbert, A., Galbraith, D., Dexter, K. G., Baker, T. R., Lewis, S. L., Meir, P., … Phillips, O. L. (2017). Biogeographic distributions of neotropical trees reflect their directly measured drought tolerances. *Scientific Reports*, *7*(1), 8334. https://doi.org/10.1038/s41598-017-08105-8

Feng, X., Porporato, A., & Rodriguez-Iturbe, I. (2013). Changes in rainfall seasonality in the tropics. *Nature Climate Change*, *3*(9), 811–815. https://doi.org/10.1038/nclimate1907

Fox, J., & Weisberg, S. (2011). *Companion to applied regression* (2nd ed.). Thousand Oaks, CA: Sage.

Gillespie, T. W., Grijalva, A., & Farris, C. N. (2000). Diversity, composition, and structure of tropical dry forests in Central America. *Plant Ecology*, *147*, 37–47. https://doi.org/10.1023/a:1009848525399

Greenwood, S., Ruiz-Benito, P., Martínez-Vilalta, J., Lloret, F., Kitzberger, T., Allen, C. D., … Jump, A. S. (2017). Tree mortality across biomes is promoted by drought intensity, lower wood density and higher specific leaf area. *Ecology Letters*, *20*(4), 539–553. https://doi.org/10.1111/ele.12748

Griffin-Nolan, R. J., Bushey, J. A., Carroll, C. J. W., Challis, A., Chieppa, J., Garbowski, M., … Knapp, A. K. (2018). Trait selection and community weighting are key to understanding ecosystem responses to changing precipitation regimes. *Functional Ecology*, *32*, 1746–1756. https://doi.org/10.1111/1365-2435.13135

Harrell Jr, F. E., & Dupont, C. (2018). *Hmisc: Harrell miscellaneous*. R package version 4.1-1. Retrieved from https://CRAN.R-project.org/package=Hmisc

Hartshorn, G. S. (1983). Plants. In D. H. Janzen (Ed.), *Costa Rican natural history* (pp. 118–157). Chicago, IL: University of Chicago Press.

Hulshof, C. M., & Swenson, N. G. (2010). Variation in leaf functional trait values within and across individuals and species: An example from a Costa Rican dry forest. *Functional Ecology*, *24*, 217–223. https://doi.org/10.1111/j.1365-2435.2009.01614.x

Johnson, M. O., Galbraith, D., Gloor, M., De Deurwaerder, H., Guimberteau, M., Rammig, A., … Baker, T. R. (2016). Variation in stem mortality rates determines patterns of above-ground biomass in Amazonian forests: Implications for dynamic global vegetation models. *Global Change Biology*, *22*(12), 3996–4013. https://doi.org/10.1111/gcb.13315

Karger, D. N., Conrad, O., Böhner, J., Kawohl, T., Kreft, H., Soria-Auza, R. W., … Kessler, M. (2017). Climatologies at high resolution for the earth's land surface areas. *Scientific Data*, *4*, 170122. https://doi.org/10.1038/sdata.2017.122

Leiva, J. A., Mata, R., Rocha, O. J., & Gutiérrez-Soto, M. V. (2009). Cronología de la regeneración del bosque tropical seco en Santa Rosa, Guanacaste, Costa Rica. I. Características edáficas. *Revista De Biologia Tropical*, *57*, 801–815. https://doi.org/10.15517/rbt.v57i3.5494

Maréchaux, I., Bonal, D., Bartlett, M. K., Burban, B., Coste, S., Courtois, E. A., … Chave, J. (2018). Dry-season decline in tree sapflux is correlated with leaf turgor loss point in a tropical rainforest. *Functional Ecology*, *32*, 2285–2297. https://doi.org/10.1111/1365-2435.13188

Martin-StPaul, N., Delzon, S., & Cochard, H. (2017). Plant resistance to drought depends on timely stomatal closure. *Ecology Letters*, *20*(11), 1437–1447. https://doi.org/10.1111/ele.12851

McDowell, N., Allen, C. D., Anderson-Teixeira, K., Brando, P., Brienen, R., Chambers, J., … Xu, X. (2018). Drivers and mechanisms of tree mortality in moist tropical forests. *New Phytologist*, *219*(3), 851–869. https://doi.org/10.1111/nph.15027

Messier, J., McGill, B. J., Enquist, B. J., & Lechowicz, M. J. (2017). Trait variation and integration across scales: Is the leaf economic spectrum present at local scales? *Ecography*, *40*(6), 685–697. https://doi.org/10.1111/ecog.02006

Millar, C. I., & Stephenson, N. L. (2015). Temperate forest health in an era of emerging megadisturbance. *Science*, *349*(6250), 823–826. https://doi.org/10.1126/science.aaa9933

Muggeo, V. M. R. (2003). Estimating regression models with unknown break-points. *Statistics in Medicine*, *22*, 3055–3071. https://doi.org/10.1002/sim.1545

Muggeo, V. M. R. (2008). Segmented: An R package to fit regression models with broken-line relationships. *R News*, *8*(1), 20–25.

O'Brien, M. J., Aviles, D. P., & Powers, J. S. (2018). Resilience of seed production to a severe El Niño-induced drought across functional groups and dispersal types. *Global Change Biology*, *24*(11), 5270–5280. https://doi.org/10.1111/gcb.14416

Oliva, J., Stenlid, J., & Martínez-Vilalta, J. (2014). The effect of fungal pathogens on the water and carbon economy of trees: Implications for drought-induced mortality. *New Phytologist*, *203*, 1028–1035. https://doi.org/10.1111/nph.12857

Peng, C., Ma, Z., Lei, X., Zhu, Q., Chen, H., Wang, W., … Zhou, X. (2011). A drought-induced pervasive increase in tree mortality across Canada's boreal forests. *Nature Climate Change*, *1*, 467–471. https://doi.org/10.1038/nclimate1293

Phillips, O. L., Aragao, L. E. O. C., Lewis, S. L., Fisher, J. B., Lloyd, J., Lopez-Gonzalez, G., … Torres-Lezama, A. (2009). Drought sensitivity of the Amazon rainforest. *Science*, *323*(5919), 1344–1347. https://doi.org/10.1126/science.1164033

Phillips, O. L., van der Heijden, G., Lewis, S. L., López-González, G., Aragão, L. E. O. C., Lloyd, J., … Vilanova, E. (2010). Drought-mortality relationships for tropical forests. *New Phytologist*, *187*(3), 631–646. https://doi.org/10.1111/j.1469-8137.2010.03359.x

Powers, J. S., Becknell, J. M., Irving, J., & Perez-Aviles, D. (2009). Diversity and structure of regenerating tropical dry forests in Costa Rica: Geographic patterns and environmental drivers. *Forest Ecology and Management*, *258*, 959–970. https://doi.org/10.1016/j.foreco.2008.10.036

Powers, J. S., & Tiffin, P. (2010). Plant functional type classifications in tropical dry forests in Costa Rica: Leaf habit versus taxonomic approaches. *Functional Ecology*, *24*, 927–936. https://doi.org/10.1111/j.1365-2435.2010.01701.x

R Core Team. (2017). *R: A language and environment for statistical computing*. Vienna, Austria: R Foundation for Statistical Computing. Retrieved from https://www.R-project.org/

Reichstein, M., Bahn, M., Ciais, P., Frank, D., Mahecha, M. D., Seneviratne, S. I., … Wattenbach, M. (2013). Climate extremes and the carbon cycle. *Nature*, *500*, 287–295. https://doi.org/10.1038/nature12350

Rodriguez-Dominguez, C. M., Carins Murphy, M. R., Lucani, C., & Brodribb, T. J. (2018). Mapping xylem failure in disparate organs of whole plants reveals extreme resistance in olive roots. *New Phytologist*, *218*(3), 1025–1035. https://doi.org/10.1111/nph.15079

Rowland, L., da Costa, A. C. L., Galbraith, D. R., Oliveira, R. S., Binks, O. J., Oliveira, A. A. R., … Meir, P. (2015). Death from drought in tropical forests is triggered by hydraulics not carbon starvation. *Nature*, *528*, 119–122. https://doi.org/10.1038/nature15539

Sala, A., Piper, F., & Hoch, G. (2010). Physiological mechanisms of drought-induced tree mortality are far from being resolved. *New Phytologist*, *186*(2), 274–281. https://doi.org/10.1111/j.1469-8137.2009.03167.x

Skelton, R. P., Brodribb, T. J., & Choat, B. (2017). Casting light on xylem vulnerability in an herbaceous species reveals a lack of segmentation. *New Phytologist*, *214*(2), 561–569. https://doi.org/10.1111/nph.14450

Smith-Martin, C. M., Xu, X., Medvigy, D., Schnitzer, S. A., & Powers, J. S. (2019). Allometric scaling laws linking biomass and rooting depth vary across ontogeny and functional groups in tropical dry forest lianas and trees. *New Phytologist*. https://doi.org/10.1111/nph.16275

Sperry, J. S., Wang, Y., Wolfe, B. T., Mackay, D. S., Anderegg, W. R. L., McDowell, N. G., & Pockman, W. T. (2016). Pragmatic hydraulic theory predicts stomatal responses to climatic water deficits. *New Phytologist*, *212*(3), 577–589. https://doi.org/10.1111/nph.14059

Stephenson, N. L., Das, A. J., Ampersee, N. J., Bulaon, B. M., & Yee, J. L. (2019). Which trees die during drought? The key role of insect host-tree selection. *Journal of Ecology*, *107*, 2383–2401. https://doi.org/10.1111/1365-2745.13176

Trugman, A. T., Detto, M., Bartlett, M. K., Medvigy, D., Anderegg, W. R. L., Schwalm, C., … Pacala, S. W. (2018). Tree carbon allocation explains forest drought-kill and recovery patterns. *Ecology Letters*, *21*(10), 1552–1560. https://doi.org/10.1111/ele.13136

Tyree, M. T., & Hammel, H. T. (1972). The measurement of the turgor pressure and the water relations of plants by the pressure-bomb technique. *Journal of Experimental Botany*, *23*(1), 267–282. https://doi.org/10.1093/jxb/23.1.267

Uriarte, M., Schwartz, N., Powers, J. S., Marín-Spiotta, E., Liao, W., & Werden, L. K. (2016). Impacts of climate variability on tree demography in second growth tropical forests: The importance of regional context for predicting successional trajectories. *Biotropica*, *48*(6), 780–797. https://doi.org/10.1111/btp.12380

Venables, W. N., & Ripley, B. D. (2002). *Modern applied statistics with S* (4th ed.). New York, NY: Springer.

Waring, B. G., Adams, R., Branco, S., & Powers, J. S. (2016). Scale-dependent variation in nitrogen cycling and soil fungal communities along gradients of forest composition and age in regenerating tropical dry forests. *New Phytologist*, *209*(2), 845–854. https://doi.org/10.1111/nph.13654

Werden, L. K., Becknell, J. M., & Powers, J. S. (2018). Edaphic factors, successional status and functional traits drive habitat associations of trees in naturally regenerating tropical dry forests. *Functional Ecology*, *32*, 2766–2776. https://doi.org/10.1111/1365-2435.13206

Wolfe, B. T., Sperry, J. S., & Kursar, T. A. (2016). Does leaf shedding protect stems from cavitation during seasonal droughts? A test of the hydraulic fuse hypothesis. *New Phytologist*, *212*(4), 1007–1018. https://doi.org/10.1111/nph.14087

Yang, Y., Saatchi, S. S., Xu, L., Yu, Y., Choi, S., Phillips, N., … Myneni, R. B. (2018). Post-drought decline of the Amazon carbon sink. *Nature Communications*, *9*, 3172. https://doi.org/10.1038/s41467-018-05668-6

SUPPORTING INFORMATION

Additional supporting information may be found online in the Supporting Information section.

How to cite this article: Powers JS, Vargas G. G, Brodribb TJ, et al. A catastrophic tropical drought kills hydraulically vulnerable tree species. *Glob Change Biol*. 2020;26:3122–3133. https://doi.org/10.1111/gcb.15037